



ELSEVIER

Fluid Dynamics Research 17 (1996) 121–145

---

---

FLUID DYNAMICS  
RESEARCH

---

---

# On the separation of droplets from a liquid jet

T.A. Kowalewski

*Center of Mechanics, IPPT PAN, Polish Academy of Sciences, PL 00-049 Warszawa, Poland*<sup>1</sup>

Received 9 March 1995; revised 22 August 1995

---

## Abstract

The droplet separation from a liquid jet was investigated experimentally. Details of the shape of the thin liquid neck joining the droplet to its parent body were studied in terms of the fluid viscosity and the jet diameter. As the viscosity increased, the neck rapidly elongated creating a long thread. Its final diameter before rupture was approximately one micrometer and seems to be constant within wide range of parameters varied. One or multiple breakups of the micro-thread were observed, which produced micro-satellites, i.e. droplets in a micrometer range. The experimental results only partly confirmed the predictions of Eggers' (Phys. Rev. Lett. 71 (1993) 3458) similarity solution. The predicted shape of the pinch-off region well overlaps the long thread observed for very viscous liquids. However, the final jet diameter, retraction velocity of the thread and presence of multiple breakups differentiate the experimental evidence from the model expectations.

---

## 1. Introduction

A liquid jet, starting as a laminar flow of liquid emerging from a circular nozzle into air, forms a cylindrical column of liquid. Due to capillary effects this liquid column is unstable and breaks down into short sections, creating droplets. This behaviour of jets has been the subject of many studies, dating back to the early investigations of Plateau (1873) and Lord Rayleigh (1878). Due to its practical importance, jet disintegration is not only a classical example of the hydrodynamic stability theory but has become a subject of several studies connected with fuel injection, ink-jet printers and fibre spinning. The vast literature on the capillary breakup of liquid jets was reviewed by Bogy (1979) and recently by Yarin (1993).

The capillary breakup mechanism predominant in small jets is associated with surface tension forces, which tend to decrease the free surface of the jet. In Rayleigh's linear limit the cylindrical jet is unstable due to a natural growth of axisymmetric disturbances. Their growth rate depends on the

---

<sup>1</sup> Most of the experiments were performed during the author's stay at the Max-Planck-Institut für Strömungsforschung, Göttingen, Germany.

jet radius and liquid properties, whereas the wavelength of the most rapidly growing disturbance  $\lambda_R$  is a simple function of the jet radius  $r_j$  only (Bogy, 1979):

$$\lambda_R = 9.02 r_j. \quad (1)$$

This inviscid, linear approximation of Rayleigh has been experimentally verified many times and found to apply remarkably well over a wide range of amplitudes of the disturbance. Also the instability growth rate deduced from the measured breakup time agrees quite well with Rayleigh's result for less viscous liquids. Liquid viscosity was introduced into Rayleigh's linear model by Weber (1931). He found that the effect of liquid viscosity is to move the most unstable wave to longer wavelengths. The wavelength  $\lambda_{We}$  of the most unstable disturbance is given as

$$\lambda_{We} = 2\pi r_j \sqrt{2 + 6(Oh/2)^{1/2}}. \quad (2)$$

A non-dimensional characteristic of the viscous effect is described by Ohnesorge number

$$Oh = \frac{\rho \nu^2}{\sigma} \frac{1}{r_j}, \quad (3)$$

where  $\rho$ ,  $\sigma$  and  $\nu$  denote density, surface tension and kinematic viscosity of liquid, respectively. For small diameter jets ( $r_j = 100 \mu\text{m}$ ) the Ohnesorge number varies from  $1.4 \times 10^{-4}$  for water to about 20 for glycerin.

Due to nonlinearities arising from inertia, capillarity and coupling of the surface kinematics to the velocity field, linear models of jet breakup have limited validity. At low and medium perturbation amplitudes there is still only one wavelength corresponding to the observed maximum growth rate of the disturbance. This has practical implication, easing control of the jet breakup, if the appropriate external excitation is applied. However, from several experimental observations (e.g. Crane et al., 1964, 1965; Donnelly and Glaberson, 1966; Goedde and Yuen, 1970; Chaudhary and Maxworthy, 1980a,b and recently Vassallo and Ashgriz, 1991), it is well known that the breakup of the jet differs in several details from the linear description. Linear theory fails completely to capture the existence of satellite drops. Also the positive and negative deformations of the jet surface are not symmetrical and the breakup does not occur at the mid-point between the two maxima.

Several nonlinear approaches were proposed, including also a direct numerical simulation. As a result, the description of the jet instability, of its breakup, and the creation of satellite droplets, were substantially improved. However, even higher order nonlinear models (Chaudhary and Redekopp, 1980) or numerical solutions (Cram, 1984) are inadequate, if we focus our attention on the spatial and temporal neighbourhood of the point at which a droplet separates from the jet (in the following called "jet tip"). This is due to the singularity which appears when the radius  $r$  of the fluid neck tends to zero. The mass of the fluid trapped in this conical region decreases as  $r^3$  but the surface force squeezing it depends only linearly on the local curvature. Hence, the singularity which appears causes most of the existing solutions to diverge, and modeling of the breakup process beyond this point is not possible. It is obvious that there must be some limiting size for jet squeezing, at least of the order of the dimension typical for the liquid molecules.

One of the first ways of approaching this problem was proposed by Keller and Miksis (1983), who considered a flow governed solely by surface tension and inertia. They argued that such a flow is self-similar with the length scale  $(\sigma t^2/\rho)^{1/3}$ , based on the surface tension, density and time  $t$ .

Peregrine et al. (1990) extended the argument introducing the viscosity of the liquid as an additional component of the length scale. Recently this idea has been completed by Eggers (1993) (also Eggers and Dupont, 1994 and Eggers, 1995), who scaled both length

$$l_\nu = \rho \nu^2 / \sigma \quad (4)$$

and time

$$t_\nu = \nu^3 \rho^2 / \sigma^2 \quad (5)$$

using only physical properties of the liquid. It is worth noticing that the length scale  $l_\nu$  appears also in the definition of the Ohnesorge number.

The flow is assumed to be axisymmetric and the  $z$  axis of a cylindrical coordinate system coincides with the axis of a liquid column. When approaching the breakup point in time ( $t \rightarrow t_0$ ), as well as in space ( $z \rightarrow z_0$ ), the diameter of the column tends to zero. Eggers (1993) looked for the asymptotic solution of this last stage of jet pinching. According to this model the asymptotic behaviour of the jet breakup is driven by some “universal” mechanisms dominating the process, independently of its previous history and geometry of the jet. Avoiding the singularity of the pinching point, the asymptotic model leaves the main question still open: is the final step of the breakup still driven by pure hydrodynamic mechanisms, or are other effects (molecular or thermal, perhaps) more important? To answer this question, more detailed observations of the pinching point are necessary.

Due to the microscopic dimensions of the pinch-off region the majority of published experimental investigations of jet instability did not consider details of the droplet detachment, limiting their field of interest to global jet characteristics for low viscosity liquids. However, according to Eggers’ predictions, details of the breakup can be easily extracted from the experiments, if the viscosity of the liquid is high enough. Proportional to the scales given by Eqs. (4), (5), the microscopic dimension of the pinch-off region should extend to a thread several millimetres long and the time scale of the process should become acceptable for experimenters. In fact, experiments performed on static elongation of a viscous droplet suspended in another immiscible liquid (Stone, 1994) indicate the creation of a thin, very long thread. Its breakup mechanism which leads to the formation of multiple satellites is remarkably similar to the capillary instability of the jet. However, in spite of the visual similarity, there are substantial differences in the boundary conditions, which do not justify quantitative comparisons of these experiments with free jet<sup>2</sup> models.

In their experiments with a small water jet in air Chaudhary and Maxworthy (1980a) have shown photographs of a long ligaments. It appeared when the fundamental frequency used for a forced breakup of the jet was disturbed by a harmonic. However, optical resolution of their apparatus and low viscosity of liquid did not allow to separate the jet structure at the breakup point.

Elongated liquid filaments have been also observed in the disintegration of non-Newtonian jets. In his monograph Yarin (1993, p.13) shows that the jet breakup of an aqueous solution of polyoxyethylene is preceded by the creation of long fluid filaments between successive jet swellings (beads-on-string). As it will be shown in the following sections, our observations indicate that a similar scenario is also present for a Newtonian liquid, if its viscosity is sufficiently high.

<sup>2</sup> Finite velocity liquid jet in vacuum or gas.

The behaviour of thin filaments created in “dripping tap”<sup>3</sup> experiments, where the droplet is formed close to the orifice, was studied by Peregrine et al. (1990) and Shi et al. (1994). Such a system differs from the free jet model. In his experimental study Kalita (1975) described the differences between the “dripping” and “jet” régimes of the drop formation. In the first case the droplet falling from the orifice creates an elongated jet, which finally breaks up. The accelerating droplet in a natural way extends the liquid thread which connects it with the orifice. Such a process, supported in addition by mechanical tension, is commonly used to obtain tiny filaments in the production of textile or optical fibres and has been extensively investigated in last decades (Ziabicki and Kawai, 1985).

Recent development of novel imaging techniques, based on CCD video cameras and image processing (Hiller et al., 1992), improved the experimental ability to record the relatively fast phenomena appearing in the small conical region of the jet tip when a droplet separates. Thus the aim of the present study was to employ modern imaging equipment to find out experimentally in what manner the droplet finally separates from the jet and to compare the observations with the predictions of the asymptotic model of Eggers (1993).

## 2. Experiments

### 2.1. Apparatus and observation methods used

The overall experimental arrangement is shown schematically in Fig. 1. It is the modified version of the apparatus used previously by Becker et al. (1991) to study droplet oscillations. The jet issues vertically downwards from the nozzle. The nozzle consists of several parts carefully machined from stainless steel and copper. It has interchangeable heads allowing the production of jets with radii in the range of 50 to 900  $\mu\text{m}$ . The pressure inside the plenum chamber of the nozzle is modulated by a piezoceramic device (Hiller and Kowalewski, 1989a). The resulting perturbations of the jet are proportional to the voltage applied to the transducer. Setting the modulation frequency close to the “natural” instability wavelength of the jet (Eq. (1)), one can obtain the periodic, perfectly reproducible breakup of the jet. Typical jet lengths were in range of 100–200 jet radii. A servo-motor traversing mechanism is used to displace the nozzle in the vertical direction. The nozzle is fed via Teflon tubes from a pressurized container, filled with the desired liquid. A special Teflon fine-mesh filter is installed at the outlet of the tank to avoid solid contaminations. It should be noted that the jet was always vertical; however the photographs are sometimes shown horizontally.

The nozzles are short ( $\approx 0.5$  mm), their length-to-diameter ratio ranged from less than 0.3 to 5, hence in practice a plug velocity profile for the issuing jet can be assumed. The speed of the jet ( $V_j$ ) is so low (a few m/s) that the flow is laminar and the effect of surrounding air is negligible ( $We \ll 1$ , where  $We = \rho_a r_j V_j^2 / \sigma$  is Weber number based on ambient gas density  $\rho_a$ ; Sterling and Sleicher, 1975). The jet velocity is yet so high that during typical acquisition time  $t_a$ , which amounts fraction of millisecond, the effects of gravitational acceleration  $g$  are unimportant ( $gt_a/V_j \ll 1$ ).

The tip of the jet was observed through a microscope lens in bright field illumination. A pulsed Light-Emitting-Diode (LED) was used as a light source (Hiller et al., 1987). Typical exposure time was below 0.2  $\mu\text{s}$ . The images of the jet were registered by a CCD camera (Sony XC77CE). Data

<sup>3</sup> Gravitationally elongated jet.

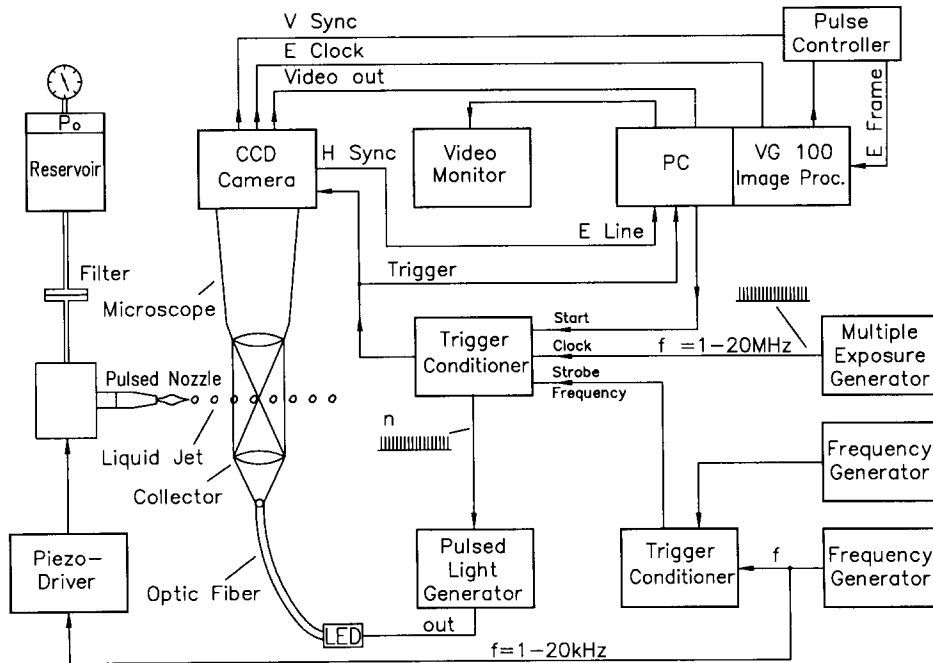


Fig. 1. Sketch of the apparatus showing the principal parts of the experimental arrangement. The Frame-Transfer configuration is shown.

acquisition and storage were performed with a 386 Personal Computer (IBM compatible) equipped with an 8-bit digitizing board VFG100 (Imaging Technology Inc.). Image processing software was used to improve the quality of the jet images as well as to measure dimensions. To determine the velocity of the jet or droplet, double exposed images were taken and the relative shift of the recorded structures was measured. For recording the temporary development of the liquid neck connecting the droplet to the jet, two novel high-speed video imaging methods were used.

The first method is based on a stroboscopic beat-frequency technique (Becker et al., 1991). A specially designed digital mixer (Hiller et al., 1989) was used to change continuously the phase of the pulses triggering the LED driver relative to the phase of the jet modulating frequency. Mixing the frequency  $F_0$  feeding the piezo driver with a phase scan frequency  $\Delta F$ , resulted in a small, well controlled frequency shift for the output signal used for the illumination. By this means, the stroboscopically observed phenomena slowly changed their phase and their development in time could be easily recorded. A new "slow motion" time base  $\Delta t_s$  scales the physical time of observed phenomena  $\Delta t$  according to a simple relation:

$$\Delta t = \Delta t_s \Delta F / 256 F_0, \quad (6)$$

where factor 256 is device construction constant. It can be seen that for a typical perturbation frequency  $F_0 = 10$  kHz, using scan frequency  $\Delta F = 1$  Hz the effective time scale can be prolonged 2560000 times. It allowed recording images at intervals  $\Delta t \geq 1 \mu s$ .

Application of this method was possible thanks to extremely high reproducibility of the excited jet perturbations. Using this technique, the images of the jet were recorded periodically by an image

processor and stored on a hard disk of the computer. Usually sequences of 200–300 images were taken. The recording time of one image was approximately 3 seconds (the time necessary to save one image on the disk). The “real time” resolution  $\Delta t$ , controlled by the scan frequency  $\Delta F$ , was kept in the range of 1–30  $\mu\text{s}$ . It allowed recording several periods of the jet breakup in one sequence of images. To avoid possible effects of external disturbances on the image quality, only one short and powerful light pulse was used to illuminate the image acquired at the selected time. This pulse was issued in synchronization with the sequence of the light pulses used for the observations. By synchronously changing the position of the camera, the development of the jet-droplet neck was followed, keeping it permanently in the field of view of the camera.

As well as acquiring images by the image processor the observed breakup was recorded on S-VHS tapes using a VCR. These images were compared with the corresponding frame grabber records to improve the accuracy of determining the pinch-off time. Theoretically the VCR recording increases temporal resolution of the stroboscopic method  $\Delta t$  by two orders of magnitude. In practice, due to the digital character of the frequency mixing, and also due to infinitesimal disturbances of the jet periodicity, the error in defining the moment of breakup is about  $0.3\Delta t$ . For the most of reported experiments, this corresponds to the range of 0.5–7  $\mu\text{s}$ .

The use of a high resolution CCD sensor ( $781 \times 584$  pixels) and precise optics allowed to obtain the spatial resolution of the stroboscopic method better than 1  $\mu\text{m}$ . This, together with its high temporal resolution makes the method favourable for investigation of the jet breakup. However, stroboscopic imaging becomes impractical if the observed process is not perfectly periodic. This may happen in the last stage of droplet separation when a thin, long neck connecting the droplet with the jet breaks up in an uncontrolled way. To facilitate observations of this phenomenon and also to verify results obtained by stroboscopic recording, a second high-speed imaging method developed by Hiller and Kowalewski (1987, 1989b) was employed.

The method is based on special features of the CCD frame-transfer camera. In full frame operation the CCD must alternate between exposure, fast transfer of charges of exposed pixel rows to a storage array, and their final readout line by line from a pixel row register. During transfer of electric charges (called frame-transfer) the CCD is still sensitive to light, so usually a mechanical shutter is used to prevent additional exposure. When operating without a shutter, image smearing will occur due to light falling on the CCD as charges are shifted (as in a classical streak camera). This effect has been used for the high speed imaging.

Initially the images were located at the top strip of the CCD array, with the remainder masked. If a strobe illumination was used during the movement of sensor charges, the first image created at the top of the CCD array moved along columns of pixels, leaving upper rows of the sensor ready for the next light pulse. Effectively a short sequences of images with small aspect ratio could be acquired filling the full height of the sensor array. Typically the charges can be shifted at speed of 1–10 lines/ $\mu\text{s}$ . Hence when the CCD was used in this way the camera effectively acquired at frame rates of several kHz. In the present experiment a specially adapted CCD sensor (Thomson TH7863 CDT) was used (Hiller et al., 1993). The sensor consists of two  $228 \times 384$  arrays of pixels, one to acquire and another to store images. Implemented modification of the frame-transfer drive-pulse allowed the use of both arrays of pixels for high-speed imaging, i.e. 456 rows each 384 pixels long were used to take one sequence of images. The minimum time necessary to transport the whole image along the columns of the sensor matrix for the device used was 160  $\mu\text{s}$ . Fig. 2 shows an example of the 8-fold sequence of images of a jet breakup taken with the use of this technique.

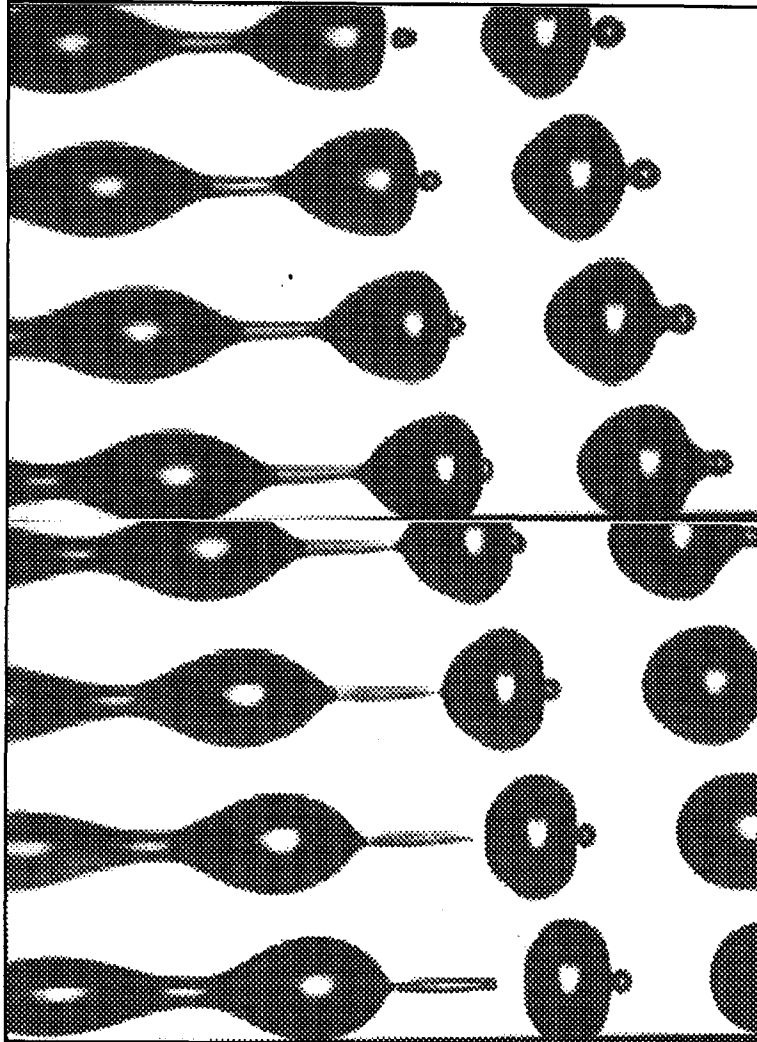


Fig. 2. The breakup of an ethanol jet. Time interval between successive images  $19.5 \mu\text{s}$ , exposure time  $200 \text{ ns}$ , nozzle diameter  $197 \mu\text{m}$ . The sequence begins from the top. The frame width corresponds to  $2.2 \text{ mm}$ .

The temporal resolution of the method depends on the number of images taken. Increasing their number allows a decrease in the time interval between images, also decreasing, however, the vertical resolution (number of rows) of a single image acquired by the camera. The horizontal resolution of the single image is that of the sensor (384 pixels). In the present investigations the sequences of 28 images of  $16 \times 384$  pixels taken at intervals  $\Delta t = 5.5 \mu\text{s}$  have typically been used to record the jet breakup. The error in defining the moment of the pinch-off is for the frame-transfer method in the worst case equal the framing interval  $\Delta t$ . To facilitate the recording procedure, the electronic system controlling the jet breakup was also used to trigger the frame-transfer camera. Applying an appropriate phase difference between the jet perturbation signal and the triggering of the camera allowed the capture at precisely the selected moment of the recorded phenomena.

Table 1  
Liquids used in the experiments and their measured physical parameters

| Liquid  | Contents | $\nu$<br>[mm <sup>2</sup> /s] | $\sigma$<br>[mN/m] | $\rho$<br>[kg/m <sup>3</sup> ] | $l_\nu$<br>[ $\mu$ m] | $t_\nu$<br>[ $\mu$ s] | $V_\nu$<br>[m/s] |
|---------|----------|-------------------------------|--------------------|--------------------------------|-----------------------|-----------------------|------------------|
| Water   | W        | 1.0                           | 72.6               | 1000                           | 0.014                 | 0.0002                | 72.7             |
| Alcohol | A        | 1.48                          | 22.5               | 803                            | 0.036                 | 0.001                 | 28.01            |
| MIXD    | G-W      | 11.24                         | 65.6               | 1161                           | 2.23                  | 0.44                  | 5.03             |
| MIXE    | G-A      | 45.0                          | 30.5               | 1081                           | 71.8                  | 114.5                 | 0.63             |
| MIXG    | G-W      | 46.0                          | 65.8               | 1209                           | 38.8                  | 32.7                  | 1.18             |
| GLY1    | G-W      | 120                           | 64.0               | 1220                           | 274.5                 | 627.9                 | 0.44             |
| GLY2    | G-W      | 180                           | 64.0               | 1230                           | 622.7                 | 2154                  | 0.29             |
| GLY3    | G-W      | 320                           | 63.8               | 1260                           | 2022                  | 12780                 | 0.16             |
| G29     | Oil      | 128                           | 31.1               | 870                            | 458.3                 | 1641                  | 0.28             |

Labels A: ethyl alcohol, W: water, G: glycerin, denote the contents of the solutions;  $\nu$ ,  $\sigma$  and  $\rho$  are the kinematic viscosity, surface tension and density;  $l_\nu$ ,  $t_\nu$  and  $V_\nu$ : scaling time, length and velocity according to Eggers' model.

The frame transfer recording suffers in vertical resolution, limiting the possibility of measuring precisely the jet diameter at the breakup point. For such measurements the stroboscopic method has been used. On the other hand, because of the high temporal resolution of the frame-transfer method and its ability to record stochastic phenomena, this method was mostly used to study the behaviour of the jet after breakup and to evaluate its retraction velocity.

## 2.2. Liquids

The investigations have been performed for water, 97% ethyl alcohol and their solutions with glycerin. This allowed a variation of the kinematic viscosity of the jet medium over the relatively wide range from  $10^{-6}$  to  $3.2 \times 10^{-4}$  m<sup>2</sup>/s. According to the asymptotic model, for such a range of viscosities the characteristic length  $l_\nu$  and time  $t_\nu$  of the breakup process (Eqs. (4), (5)) change by several orders of magnitude.

Table 1 collects the physical parameters of the liquids used, together with the corresponding scaling values of Eggers' model. The scaling velocity  $V_\nu = l_\nu/t_\nu$  is also given for convenience. The listed physical values have been carefully measured at the temperature 295 K using standard methods.

The investigations have been performed with the liquid jet emerging to the normal atmosphere at room temperature (295 K). To investigate possible effects of the surrounding gas on the breakup process, some experiments have been also performed at low ambient pressure (100 Pa). For these experiments the low vapour pressure oil (Shell G29) was used as the jet medium.

## 2.3. Results

Fig. 2 shows a typical sequence of the jet breakup for low viscosity liquids. It can be seen that before the droplet separates, a long liquid ligament is created, connecting the jet swell with the preceding droplet. The length and diameter of this structure, in the following called "macro-thread", is a function of the liquid viscosity and the nozzle diameter. It depends also on the jet perturbation amplitude and frequency. After the breakup the macro-thread separates from the parent jet creating

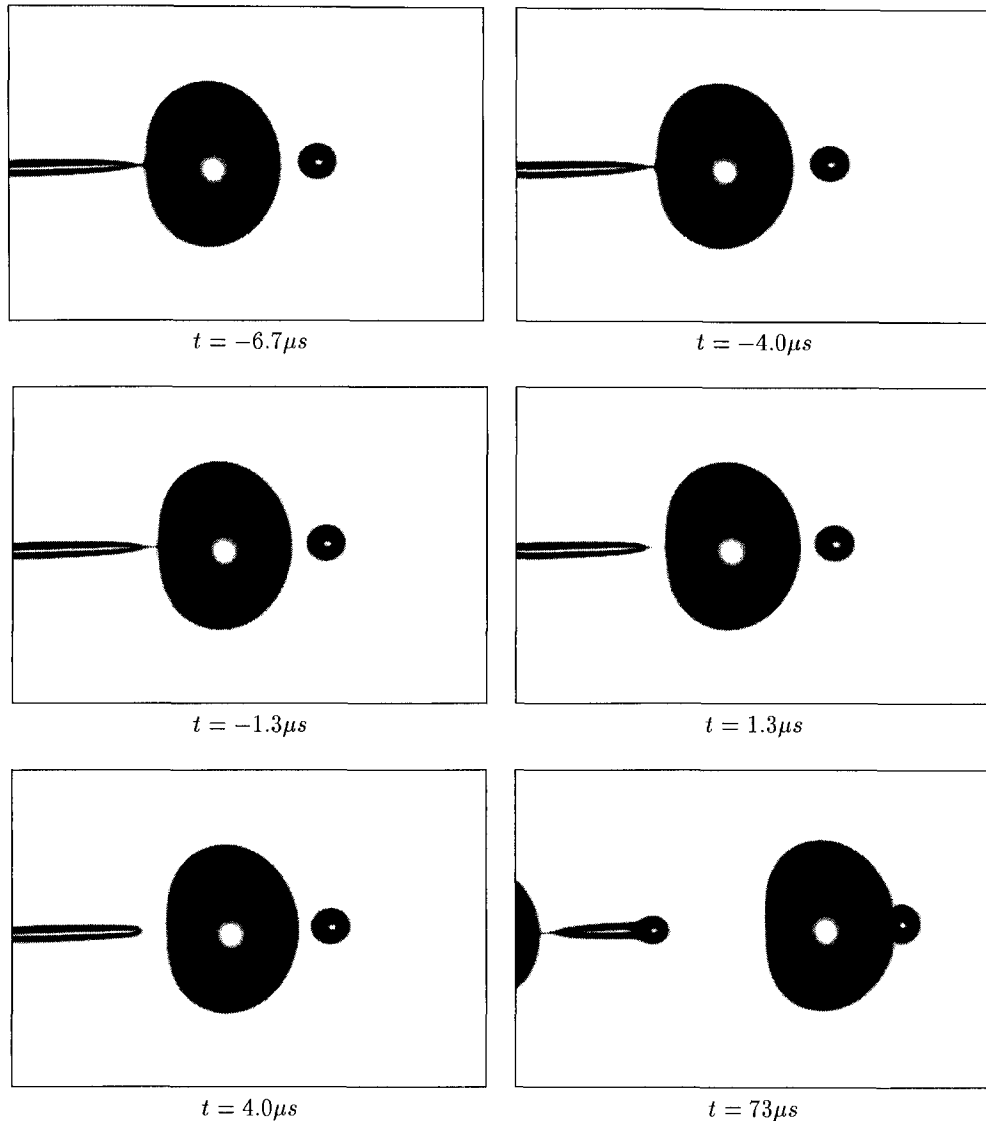


Fig. 3. Separation of the droplet from the liquid jet of radius  $r_j = 98.5 \mu\text{m}$ . Time is given relative to the moment of the jet breakup. Liquid medium of relatively low viscosity (MIXD). The width of one frame corresponds to 1 mm

a satellite droplet. Apparently, the breakup is initiated by an abrupt shrinking of the macro-thread diameter in the region where it connects with a droplet. Increasing the medium viscosity, it is possible to make this region more clearly visible. A sequence of jet images shown in Fig. 3, taken for the liquid of relatively low viscosity (MIXD), shows already more details of the breakup region. Only part of the macro-thread, the diameter of which is a fraction of the parent jet diameter, is shown in the left side of the images. Following the sequence it can be observed that several milliseconds before the macro-thread breaks, its tip elongates approaching a conical form. Shortly before the rupture, a fine secondary filament emerges, which connects the macro-thread with the droplet. It can be clearly

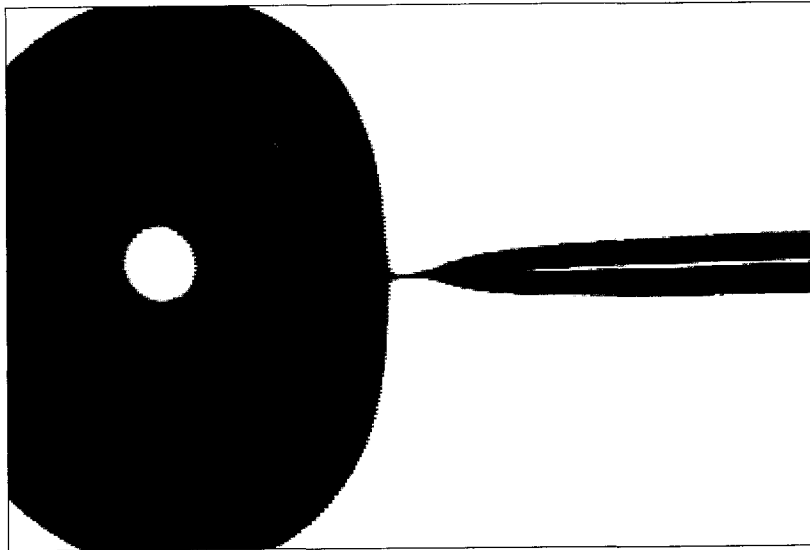


Fig. 4. Enlargement of the breakup region at  $1.3 \mu\text{s}$  before the droplet separation (compare Fig. 3). Creation of the tiny micro-thread. The frame width corresponds to  $0.5 \text{ mm}$ .

seen in the enlargement shown in Fig. 4. Immediately after the rupture of the jet-droplet filament, its remnant rapidly moves back to the parent jet. This is due to the surface tension, which, because of the large curvature of the thread tip, quickly accelerates it back to the issuing nozzle. The surface disturbances of the main jet propagating in the opposite direction interfere with the shrinking macro-thread, causing its secondary breakup and generation of a satellite droplet. As can be seen in the last image of Fig. 3 ( $t = 73 \mu\text{s}$ ), creation of the satellite droplet shows a substantial similarity to the process observed for the main droplet. The elongated end of the macro-thread creates a thin filament, shortly before this whole structure separates from the parent jet to become the satellite droplet. All typical characteristics of the process, i.e. the length and diameter of the neck, as well as its retraction velocity, are similar to the corresponding values observed for the separation of the main droplet.

The order of magnitude of the minimum diameter of the “micro-thread” is the same as that of the optical resolution of the system, i.e.  $\approx 1 \mu\text{m}$ . At the moment it is hard to say whether any subsequent degradation of the liquid neck takes place before the droplet fully separates. However, experiments described below performed using more viscous liquids seem to confirm that this is the lower limit of the micro-thread diameter. We believe this, because the micro-thread can be well seen both shortly before and also after the pinch-off. Hence, except for an infinitesimal region around the breakup point, the rest of the micro-thread to be visible must preserve its final diameter of the order of  $1 \mu\text{m}$ . The point of the neck breakup is located about  $3\text{--}5 \mu\text{m}$  from the droplet surface.

The main parameters monitored for the investigated jets were: the retraction velocities of both the macro- and micro-thread (denoted  $V_{21}$  and  $V_{22}$ ), the variation in time of the length of the micro-thread (defined as a distance  $L(t)$  from the end of the macro-thread to the droplet surface), the variation in time of the minimum diameter of the neck  $d(t)$ , and also the location of  $d(t)$  relative to the droplet. The range of variation of the dimensional values of the measured characteristics is relatively wide, depending on the viscosity of the liquid. The sequence of images (Figs. 5–8), taken for more viscous liquids, demonstrates how viscosity affects the pinch-off region.

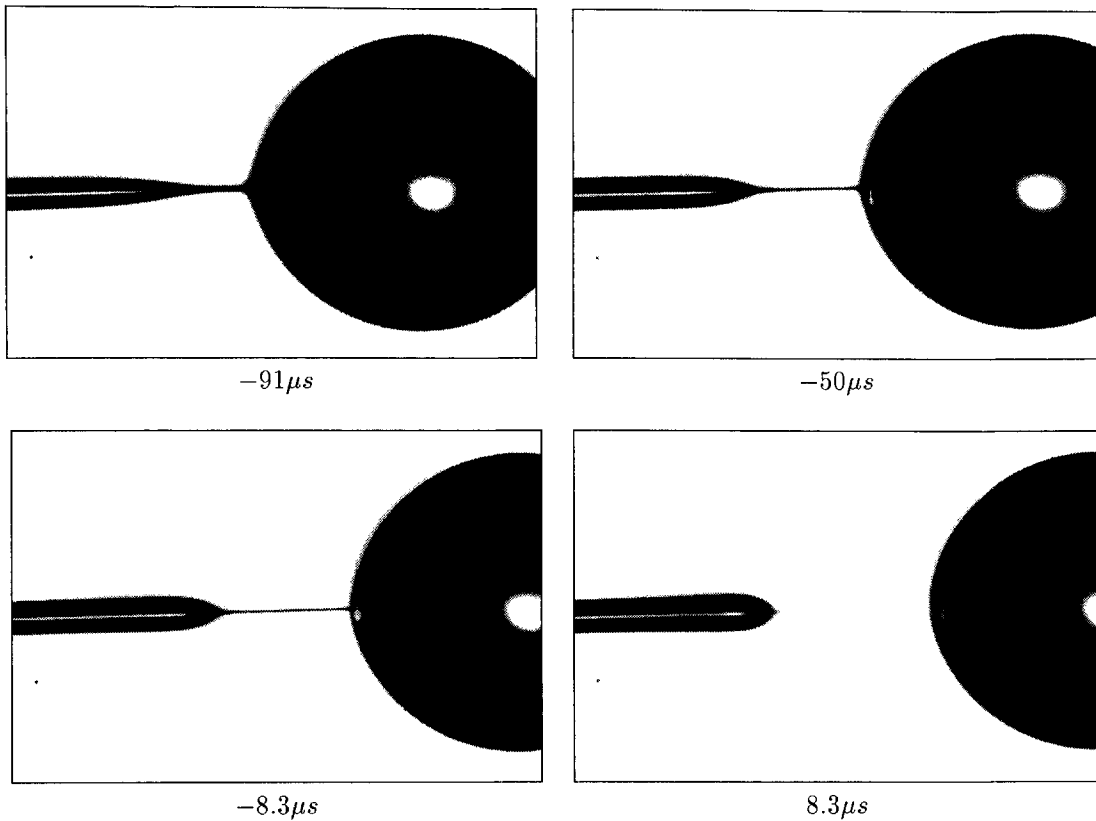


Fig. 5. Separation of the droplet for higher viscosity of liquid (MIXE). The jet radius  $r_j = 140\ \mu m$ . Time relative to the moment of neck rupture. The width of one frame is 1 mm.

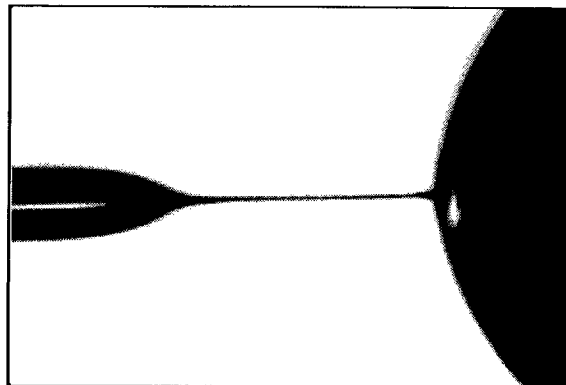


Fig. 6. Enlargement of the breakup region at  $16.6\ \mu s$  before the rupture (compare Fig. 5). Tiny micro-thread forming the neck between macro-thread and droplet well seen. The frame width corresponds to 0.5 mm.

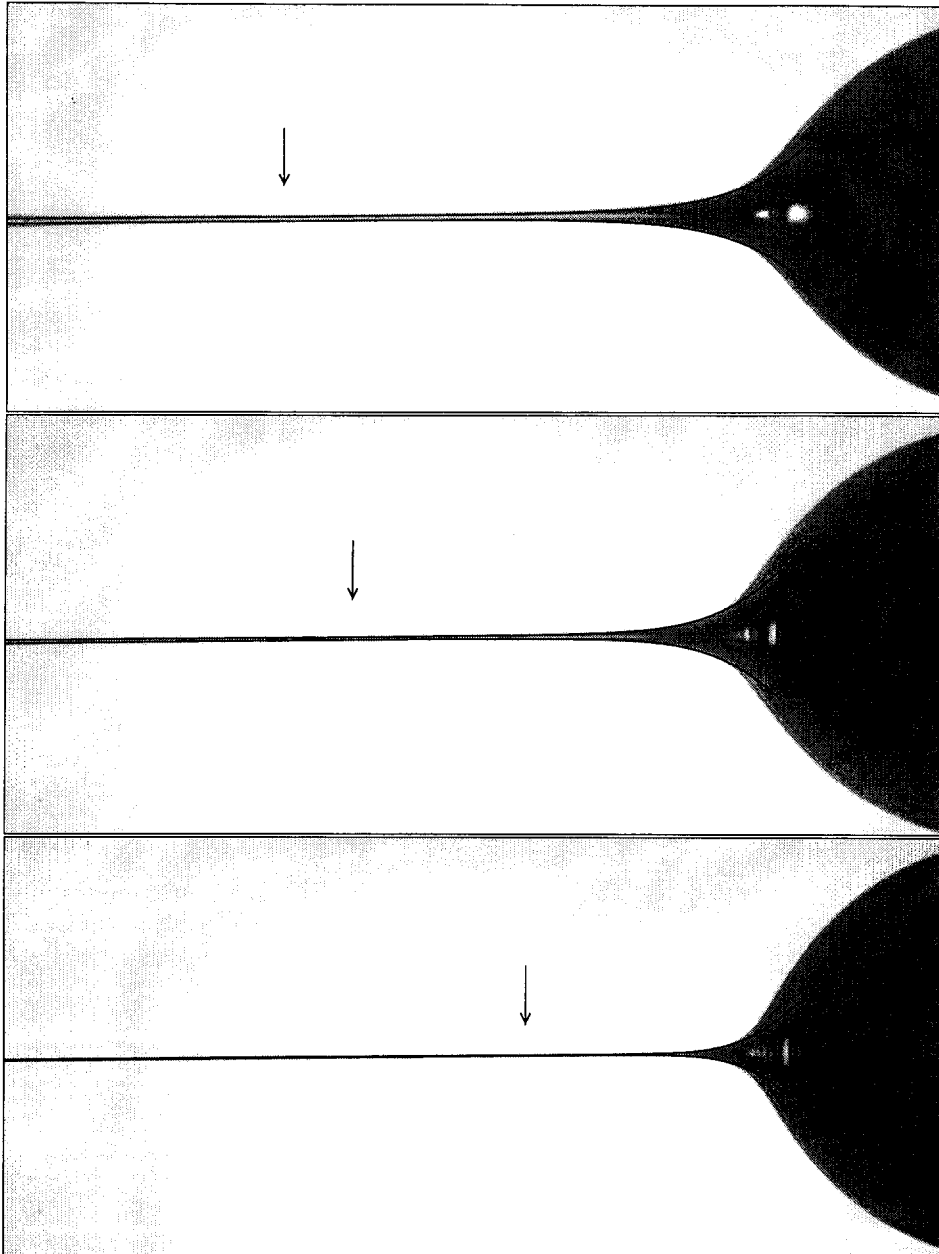


Fig. 7. Process of the droplet separation observed for the jet of radius  $r_j = 195 \mu\text{m}$ ; liquid medium of high viscosity (GLY3). The drawn line denotes the predicted shape of the neck calculated according to Eq. (8). The arrows indicate location of the function minimum. Time (from the top) relative to the moment of rupture:  $-1053 \mu\text{s}$ ,  $-614.6 \mu\text{s}$  and  $-175.6 \mu\text{s}$ . The frame width corresponds to 2 mm.

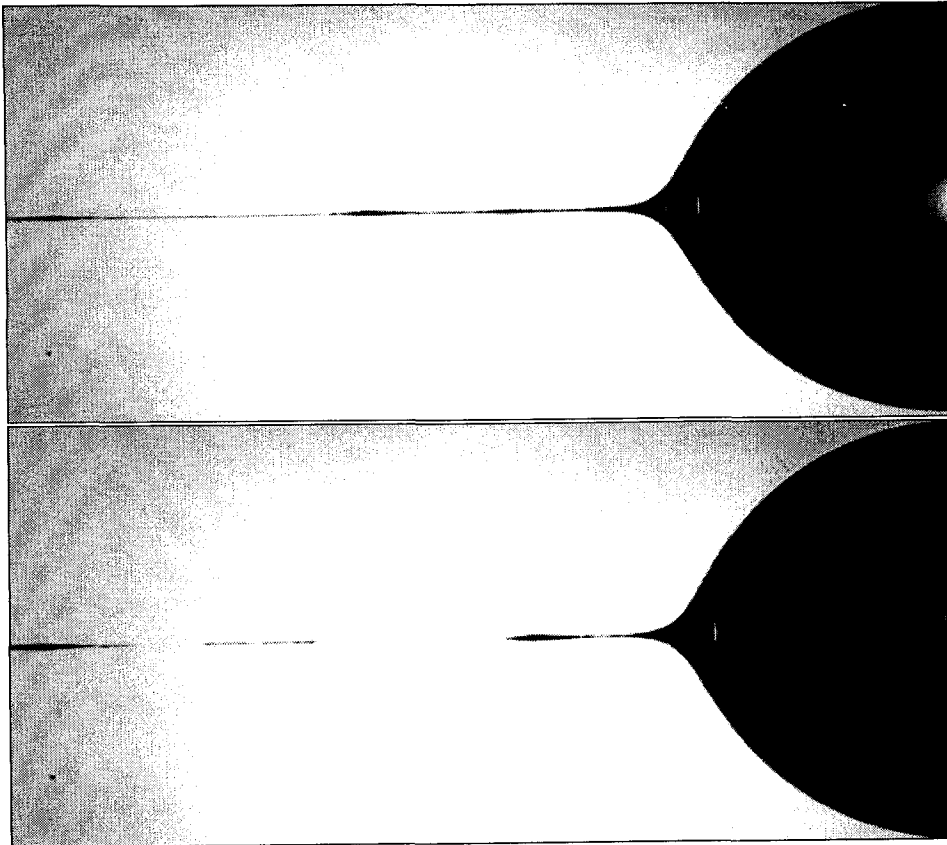


Fig. 8. Continuation of the sequence from Fig. 7. The moment of breakup of the micro-thread and  $44 \mu\text{s}$  later.

In the left part of Fig. 5 the elongated end of the macro-thread which shrinks into a thin micro-thread can be well identified. The micro-thread is visible as a long filament of about one micrometer diameter, the length of which reaches almost 0.3 millimetres at the moment of pinch-off. Close to the droplet ( $\approx 3\text{--}4 \mu\text{m}$ ) the micro-thread abruptly grows in diameter and smoothly merges into the droplet surface (Fig. 6). Similar behaviour can be observed for a very viscous liquid (GLY3) in Figs. 7, 8. However, now the micro-thread reaches a length of several millimetres and its other end, connecting to a macro-thread, cannot be shown in the scale of the figure. Shortly before the droplet separates from the micro-thread several small perturbations of its diameter appear, followed by multiple pinch-offs.

The micro-thread elongation and rupture can be well followed in the sequence of images taken with help of the frame-transfer camera and shown in Fig. 9. In contrast to the previous images taken with help of the stroboscopic method, the process of the drop separation is recorded in real time, i.e. the images correspond to a single sequence of the jet breakup. Generally there are no large differences between the images taken with both methods of recording. This confirms the high reproducibility of the phenomena. Only the last stage of the process, the disintegration of the thin liquid thread exhibits some stochastic behaviour. Short before the micro-thread breaks up, small-amplitude perturbations start to grow (Fig. 9), leading to multiple pinch-offs. The phenomena indicate some similarity to

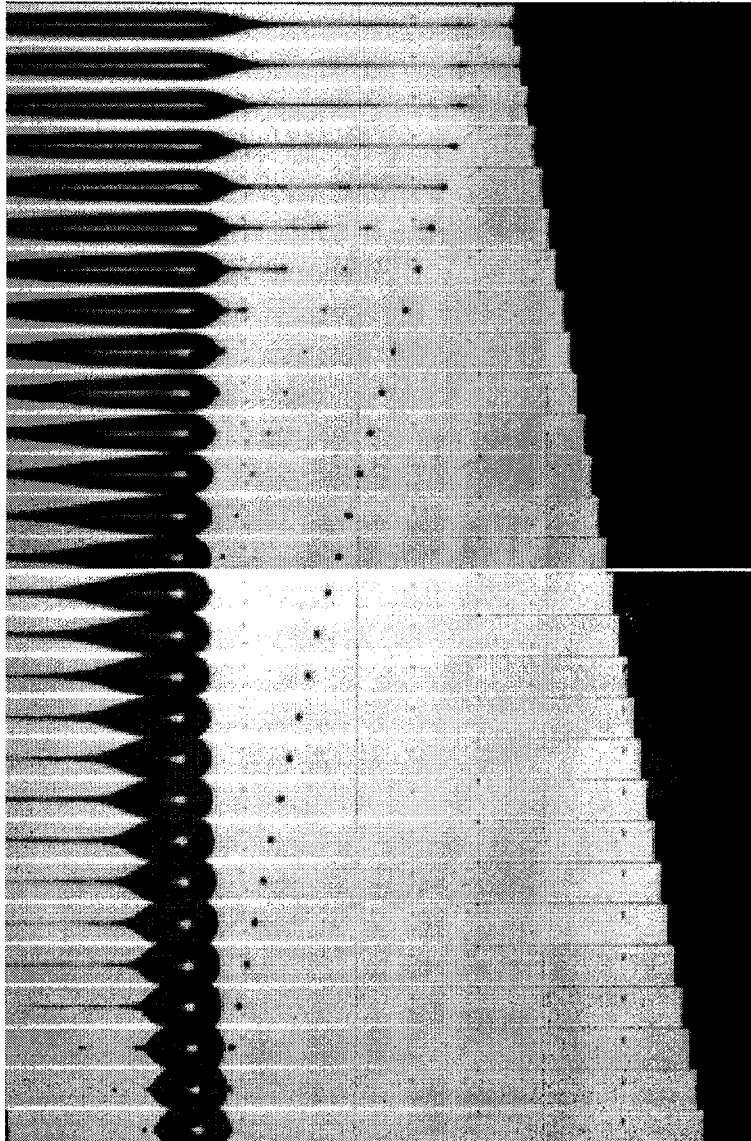


Fig. 9. The droplet separation observed for the jet of radius  $r_j = 250 \mu\text{m}$ ; generation of micro-satellites. Liquid medium of higher viscosity (MIXG); time interval  $5.5 \mu\text{s}$ . The frame width corresponds to 1.1 mm. Images taken by the Frame-Transfer method.

the well known capillary instability of a large scale jet. Similar to the typical disintegration of a liquid column, small micro-satellites are created from swellings of the micro-thread (Figs. 8 and 9). However, there is no indication that there is one characteristic wavelength of the perturbations, corresponding to the maximum growth rate of the linear stability theory. For the typical diameter of the micro-thread of 1 to  $3 \mu\text{m}$ , the distance between the created swellings is orders of magnitude larger than that predicted for Rayleigh instability (Eq. (1)). It is possible that the capillary instability

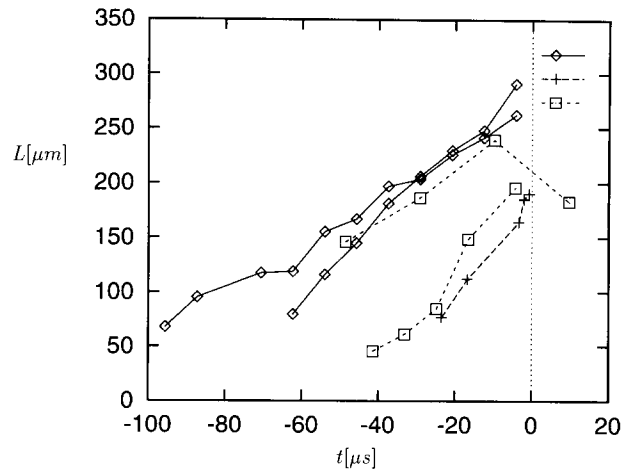


Fig. 10. Length of the micro-thread  $L$  as a function of time measured relative to the moment of rupture. Experiments:  $\diamond$ : liquid MIXE  $r_j = 140 \mu\text{m}$ ,  $+$ : MIXG,  $r_j = 37.5 \mu\text{m}$ ,  $\square$ : MIXG,  $r_j = 98.5 \mu\text{m}$ .

of the micro-thread is strongly modified by its elongation as well as by dominant effects of viscosity and surface tension.

Observing carefully images taken by the “Frame-Transfer” method (Fig. 9) one may find another striking regularity of the process of droplet separation. In the fixed frame of reference connected with the camera, the relative retraction velocity of the macro-thread ( $V_{z1}$ ) in several frames is close to zero. Hence, during this period of time the macro-thread retraction velocity is constant and equals the jet velocity (the emanating velocity  $V_j$ ). It is difficult to find any explanation of this strange correlation, observed for a relatively wide range of experimental parameters.

In order to find out if the pressure of the surrounding gas might influence the breakup process, experiments have been performed for the jet of oil (system G29) emanating from the nozzle into a container filled with air at normal (100 kPa) and low pressure (100 Pa). There was no evidence of the effect of external pressure. Neither the retraction velocities nor the length of the micro-thread, nor the whole scenario of the breakup were changed. In both cases, i.e. at the low and normal environment pressures, the micro-thread has shown similar capillary instability with one or several pinch-off points leading to creation of the micro-satellites.

#### 2.4. Analysis of observations

Looking at sequences of images acquired in the present investigation one can isolate two main phases of the breakup process. First, a very pronounced neck on the main jet surface develops in the macro-thread close to the droplet. The diameter of the macro-thread, which depends on the parent jet diameter, is relatively large (0.1–0.5 mm). At a later stage, the conical portion of the macro-thread begins elongating and thinning the neck. Due to the increased action of surface tension, fluid is pumped out of the neck. Consequently, the neck diameter continues thinning and within a short time a new cylindrical micro-structure of liquid is created, connecting the macro-thread and the droplet. When the diameter of this new micro-thread falls below a few micrometers, further outflow of the viscous liquid is damped. At this point the second phase of the breakup begins. Thinning of the micro-

thread slows down. The flow of liquid back to the macro-thread becomes insufficient to compensate for the created pressure difference; the surface force acting at the conical ending begins to contract it. In consequence a pulling force is created which elongates the micro-thread connected on the other side to the large, inert droplet. The observed growth of the micro-thread length is approximately linear in time. It is illustrated in Fig. 10, which shows the length of the micro-thread as measured in a few experimental runs.

The images of the jet breakup taken for the low viscosity liquids show only a small narrowing of the neck close to the droplet (Fig. 4). The short length of the micro-thread does not allow for the growth of the capillary waves and the rupture point is relatively well defined. With increased viscosity the outflow of liquid from the neck is strongly damped and the process of neck pulling takes place. The length of the created thread may reach up to several hundreds diameters, and its breakup often leads to multiple pinch-offs. It was therefore not possible to correlate the location of the rupture point with the experimental parameters.

The main results of the observations have been summarized in Table 2. It collects the breakup characteristics measured within a time interval  $\Delta t$  from the moment of rupture. The interval  $\Delta t$  is the period of image recording. It limits the accuracy of estimating the moment of the droplet separation, and hence the accuracy of the presented maxima of the micro-thread length and the velocities of retraction. As was mentioned before, this accuracy is estimated to be  $0.3\Delta t$ . The two retraction velocities measured are the macro-thread velocity  $V_{z1}$  at the conical end and the micro-thread velocity  $V_{z2}$  at the point of the pinch-off.

The velocities of retraction are given for an observer moving with the jet velocity. Therefore, in the first step of the evaluation procedure, the translation velocity of the jet-droplet system had to be estimated. For the sequence of images with a well visible droplet, its centre of mass has been evaluated by the method given elsewhere (Becker et al., 1991). The translational velocity of this point has been taken as the reference. Small dimensions of the jet and short time of the experiment justified the assumption that for one sequence of images this velocity remains constant. For viscous liquids both retraction velocities are given:  $V_{z1}$  is the retraction velocity of the well visible macro-thread emerging from the main jet, and  $V_{z2}$  the retraction velocity of the micro-thread. The last one is essential for the description of the jet rupture, as this is the retraction velocity which emerges in modeling the last stages of the pinch-off process. At the low viscosity range, it is almost impossible to distinguish between the end of the macro-thread and the micro-thread, and therefore only one value of the retraction velocity is given.

The small dimension of the micro-thread and the inaccuracy of catching the breakup time allow only for an estimation of its initial retraction velocity. However, measurements based on the present observations have not indicated any considerable acceleration of the contracting micro-thread. The macro-thread begins to contract, elongating the micro-thread well before the breakup. At the pinch-off time the macro-thread velocity is almost constant, and reduces when it begins to form a spherule.

The results collected in Table 2 confirm the already mentioned strong dependence of the maximum length of the micro-thread ( $L_{\max}$ ) on the liquid viscosity. The length ( $L_{\max}$ ) changes over three decades, from micrometers for less viscous liquids to millimetres for the highly viscous solution of glycerine (GLY3). On the other hand the dependence of the retraction velocity on the viscosity is less apparent. The measured values of the micro-thread velocities being of the order of  $10\text{m/s}$ , show relatively large scatter, difficult to systematize on the basis of the parameters of the liquid. Probably such parameters as jet diameter and the issuing velocity may modify the observed contraction

Table 2

Typical characteristics of the jet breakup observed within a time interval  $\Delta t$  before (after) the rupture

| Liquid             | $r_j$<br>[ $\mu$ m] | $F_0$<br>[Hz] | $\Delta t$<br>[ $\mu$ s] | $L_{\max}$<br>[ $\mu$ m] | $L_{\max}/l_\nu$<br>– | $d_{\min}$<br>[ $\mu$ m] | $V_{z1}$<br>[m/s] | $V_{z2}$<br>[m/s] | $V_j$<br>[m/s] |
|--------------------|---------------------|---------------|--------------------------|--------------------------|-----------------------|--------------------------|-------------------|-------------------|----------------|
| W <sub>FT</sub>    | 48                  | –             | 5.5                      | < 1                      | –                     | < 1                      | –                 | 6.5               | 1.9            |
| A                  | 98.5                | 7840          | 1.6                      | < 1                      | –                     | < 1                      | –                 | 10.0              | 5.6            |
| MIXD               | 98.5                | 4337          | 2.66                     | 45                       | 20.1                  | 0.7                      | 2.4               | 4.9               | 2.9            |
| MIXE               | 140                 | 1391          | 8.3                      | 294                      | 4.09                  | 0.7                      | 2.3               | 24                | 2.1            |
| MIXG               | 37.5                | 8625          | 1.34                     | 220                      | 5.67                  | < 1.2                    | 6                 | 30                | 5.3            |
| MIXG <sub>FT</sub> | 37.5                | 7723          | 5.55                     | 220                      | 5.67                  | –                        | 4.5               | 25                | 4.5            |
| MIXG               | 98.5                | 1401          | 8.28                     | 250                      | 6.44                  | 0.7                      | 2.1               | 10.6              | 1.91           |
| MIXG <sub>FT</sub> | 98.5                | 2590          | 5.55                     | 380                      | 9.8                   | –                        | 3.4               | 8.8               | 3.4            |
| MIXG <sub>FT</sub> | 190                 | 775           | 19.45                    | 400                      | 10.3                  | –                        | 2.3               | 5.5               | 1.7            |
| MIXG <sub>FT</sub> | 250                 | 2852          | 5.55                     | 380                      | 9.8                   | –                        | 2.0               | 5.0               | 1.9            |
| MIXG <sub>FT</sub> | 650                 | 75            | 19.45                    | 250                      | 6.44                  | –                        | 0.3               | 8.0               | 0.33           |
| MIXG               | 650                 | 73            | –                        | 350                      | 9.02                  | 0.7                      | –                 | –                 | 0.95           |
| GLY1               | 195                 | 380           | 15.1                     | 860                      | 3.13                  | 0.7                      | 1.0               | 4.0               | 0.65           |
| GLY2               | 900                 | 85            | 137                      | 1420                     | 2.28                  | 0.7                      | 1.6               | 4.3               | 1.92           |
| GLY3               | 195                 | 603           | 10.97                    | 1750                     | 0.86                  | 0.7                      | –                 | –                 | 1.4            |
| GLY3 <sub>FT</sub> | 195                 | 553           | 5.5                      | 1800                     | 0.89                  | –                        | –                 | 13.0              | 1.2            |

$L_{\max}$  is the maximum length of the micro-thread,  $d_{\min}$  its minimum diameter,  $V_{z1}$ ,  $V_{z2}$ , the retraction velocity of the macro- and micro-thread. Experimental runs with a subscript FT were recorded using the Frame-Transfer technique.  $F_0$  is the jet excitation frequency (run W<sub>FT</sub> realized using “drop on demand” device).

velocities. For example, the data for the system MIXG for the small diameter nozzle (75  $\mu$ m) show an evident increase of the retraction velocity  $V_{z2}$ , compared to the measurements for the larger nozzles. One of the possible reasons for this deviation is the difference in the droplet-jet configuration. For small diameter jets the distance between neighbouring jet swellings becomes comparable to the length of the micro-thread. Hence, the thinning of the macro-thread begins almost symmetrically from both sides, finally leaving only its small portion in the middle. Then, the pinch-off of the two symmetrical micro-threads begins almost simultaneously.

The present results have shown that at the last stage of the jet breakup, the micro-thread, a thin liquid filament connecting the parent jet structure with the departing droplet, is created. This new structure of the breakup process, as well as the micro-satellites created afterwards, are invisible in low resolution optical observations. It should therefore be noticed that in the majority of the earlier experiments, for example reports by Chaudhary and Maxworthy (1980a,b) and Goedde and Yuen (1970), this micro structure was not observed for the previously mentioned optical reasons. Only the microscopic imaging from small distance made it possible to identify this new element of the jet breakup process. Therefore, one should distinguish the present data on the diameter and velocity of the micro-thread from the values reported in the literature, which usually correspond to the well seen elongated part of the macro-thread. For the same reason the real moment of jet rupture is slightly delayed as compared to the macroscopic observations.

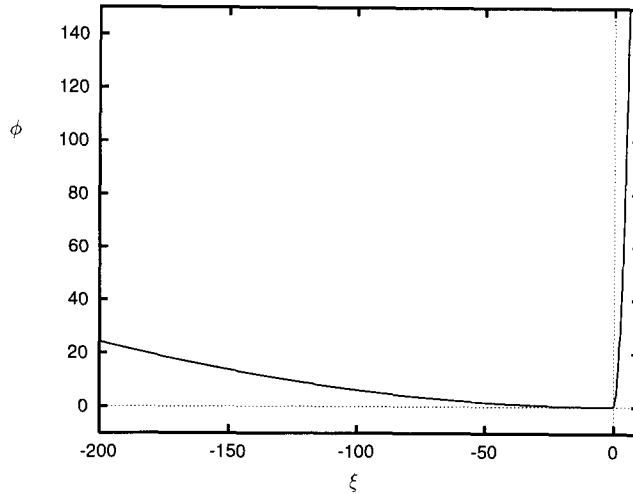


Fig. 11. Nondimensional function  $\phi(\xi)$  describing the jet shape at the breakup point (Eggers, 1993).

### 3. Eggers' model of jet pinch-off

Starting from the Navier-Stokes equations for an axisymmetric column of fluid Eggers (1993) derived a simple one dimensional description of the last stage of the jet pinching. The usefulness of a one-dimensional, asymptotic analysis for describing stability of the liquid column has been extensively explored by Schultz and Davis (1982) and Schultz (1987) in their studies of liquid fibres. The main idea is based on the assumption that far from the jet "ends" the lowest order expansion in terms of the radial coordinate applies. In Eggers' case the pinch-off radius became the expansion parameter. This allowed him to reduce the problem to a coupled set of ordinary differential equations for two scaled functions  $\phi(\xi)$  and  $\psi(\xi)$ . A similarity variable  $\xi$  characterizes the distance from the breakup point  $(t_0, z_0)$ :

$$\xi = \frac{z - z_0}{l_v} \sqrt{t_v / (t_0 - t)}. \quad (7)$$

The shape of the jet surface  $y$  and its velocity  $v$  can be easily found using solutions for  $\phi(\xi)$  and  $\psi(\xi)$ , respectively:

$$y(z, t) = l_v(t_0 - t) / t_v \phi(\xi), \quad (8)$$

$$v(z, t) = l_v / t_v \sqrt{t_v / (t_0 - t)} \psi(\xi). \quad (9)$$

This result has very important consequences. Independent of macroscopic initial conditions, the final shape and velocity of the jet tip are given by two universal functions  $\phi$  and  $\psi$  respectively, scaled only by the coefficients  $l_v$  and  $t_v$ . Fig. 11 shows the shape function  $\phi(\xi)$ , obtained by Eggers.

In the preceding section it has been shown that the viscosity of the liquid has an essential significance for the process of the droplet separation. Of course the surface tension and density of the liquid, and geometrical parameters of the experiment may also play a role, but unfortunately their variation in the performed experiments was relatively small. Let us first systematize the measurements in terms of the characteristic time and length scales. Among the parameters of the experiment there

are three independent length scales which characterize the hydrodynamics of the jet: the diameter of the nozzle,  $D \approx 2r_j$ , the capillary length  $l_c = \sqrt{\sigma/\rho g}$  and the viscous length  $l_\nu$  (Eq. (4)). In the performed experiments it was not possible to find any evidence that the jet diameter has significant influence on the pinch-off process. The final scenario of the droplet separation is very similar for both small and large diameter nozzles used. Also the capillary length does not seem to be a suitable scale as it does not include viscosity. Hence, the measured dimensions are scaled using the remaining viscous length, which seems most appropriate to describe the observed effects of viscosity. Following Eggers' model we take also the viscous time  $t_\nu$  (Eq. (5)) to scale time. Then, the two retraction velocities will also be scaled with  $V_\nu = \sigma/\nu\rho$ . Values of the scaling factors for the fluids used can be found in Table 1.

Table 2 collects the values of the characteristic dimensions measured for the micro-thread when the droplet separates. It seems that selection of  $l_\nu$  as the length scale gives some ordering of the maximum lengths of the micro-thread ( $L_{\max}$ ) for various viscosities. In most of the cases the non-dimensional length of the micro-thread ( $L_{\max}/l_\nu$ ) stays in the range 4–10. However, outside this range there are values corresponding to measurements done at the highest (GLY3) and the lowest (MIXD) limits of the viscosity of the liquid. Also, within the same liquid system (e.g. MIXG) the length of the micro-thread measured for the different experimental runs varies by almost 100%. We must conclude that, although the selected scale properly highlights the observed correlation between the micro-thread length and the medium viscosity, there are still some missing parameters in the description. It is not surprising, since the model describes only the pinch-off region and its validity is limited to  $z/l_\nu < 1$ .

The Eggers' model (Eggers, 1993 and 1995) predicts also non-dimensional values of the maximum retraction velocity  $V_{\max}$  and the minimum diameter  $d$  of the neck at a given time:

$$V_{\max}(t) = 8.726\sqrt{\nu}/\sqrt{(t-t_0)}, \quad (10)$$

$$d(t) = 0.0608(\sigma/\rho\nu)(t_0-t) = 0.0608V_\nu(t_0-t). \quad (11)$$

Observing the minimum diameter of the micro-thread given in the Table 2 we can see that its value ( $\approx 1 \mu\text{m}$ ) is in practice constant in all experiments and scaling it with  $l_\nu$  has no meaning. The same applies to the retraction velocities. The non-dimensional velocity values obtained when using  $V_\nu$  (Table 1) did not show any clear improvement of ordering, both for the tip velocity of micro-thread ( $V_{z2}$ ), and for the velocity of the end of the macro-thread ( $V_{z1}$ ). On the contrary, their dimensional values are characterized by much lower spread. Equation (10) shows that the predicted retraction velocity should be a function of time and viscosity only. This is a surprising result, as intuitively we would expect that velocity should depend on the main "natural" parameters, namely the surface tension, the density and the neck curvature. Correlating the velocity of the micro-thread with the almost constant pinch-off diameter  $d_{\min}$  we obtain at least some explanation of why its value does not change very much in the experiments. In fact, for typical liquid density  $\rho = 1000 \text{ kg/m}^3$ , surface tension  $\sigma = 50 \times 10^{-3} \text{ N/m}$  and micro-thread diameter  $d_{\min} = 1 \mu\text{m}$ , its retraction velocity is of the order of  $\sqrt{\sigma/\rho d_{\min}}$ , i.e. 10 m/s. This agrees with the range of the observed values of  $V_{z2}$ . The data shown in Table 2 reveal also that the micro-thread retraction velocity  $V_{z2}$  does not depend significantly on the liquid viscosity. Hence, within the observed data scatter it is not possible to justify the relation (10). On the other hand, because of the almost constant diameter of the micro-thread

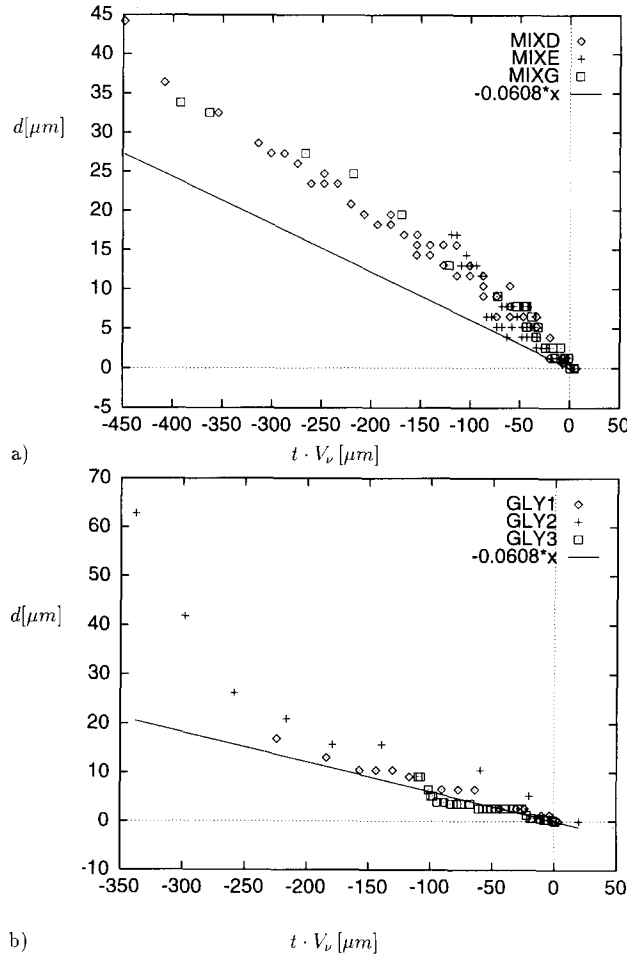


Fig. 12. Measured variation in time of the minimum jet diameter before the droplet separation, compared with the linear relation given by Eq. (11). (a) Experiments performed for less viscous liquids (MIXD, MIXE, MIXG); (b) Highly viscous liquids (GLY1, GLY2, GLY3)

and the relatively small variation of the surface tension within the systems tested, it is difficult to correlate the velocity data with these parameters.

According to Eq. (11) the minimum diameter of the neck  $d$  is a linear function of time. Fig. 12 shows a comparison of the model prediction with the measured behaviour with time of the micro-thread diameter. The validity of the asymptotic model is limited to the pinch region, i.e.  $t/t_v < 1$ ,  $z/l_v < 1$ . In Fig. 12, this region corresponds to the abscissa values smaller than  $l_v$ . In fact, for less viscous liquids (Fig. 12a) this length corresponds only to a small section of the abscissa ( $l_v \leq 50 \mu\text{m}$ ) and the measured data apparently differ from the predicted relation. For more viscous liquids the length scale  $l_v$  covers the range 274–2022  $\mu\text{m}$ , and as is shown in Fig. 12b, the experimental data correspond quite reasonably to the model prediction.

As we said in the introduction, the Eggers' asymptotic model predicts a universal shape of the pinch-off region using only one function  $\phi(\xi)$  (Fig. 11). The flat part of the function for  $\xi < 0$

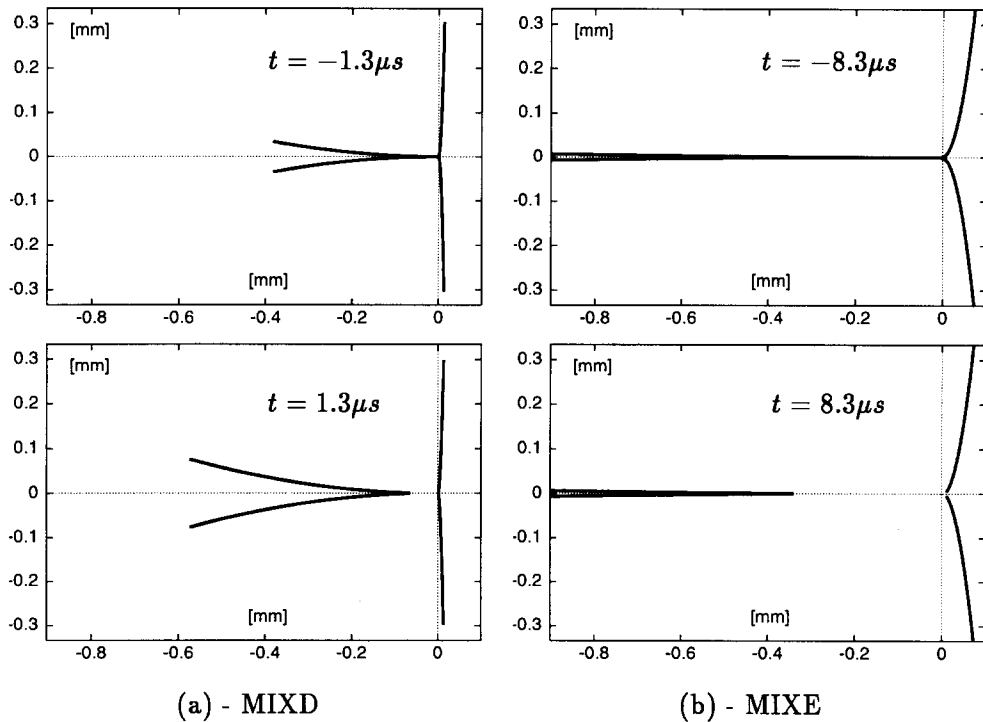


Fig. 13. Predicted shape of the pinch-off region according to Eggers' model, to be compared with the observed micro-threads in Fig. 3a and Fig. 5b. The plots are scaled to match physical dimensions in the above mentioned images of the jet. Time is given relative to the pinch-off moment.

relates to the observed micro-thread. Depending on the scaling values  $(t_v, l_v)$ , a longer or shorter part of the function around the singularity  $\xi = 0$  may be used to describe the physical phenomena. This is in general agreement with the present experiments showing that the micro-thread length increases with the fluid viscosity.

Fig. 13 shows some examples of the predicted jet shape as calculated for the experimental parameters of the observed micro-threads and displayed in Figs. 3 and 5 (systems MIXD and MIXE). The Eggers' approximation is based on the small parameter expansion; hence the comparison with experiments is justified only around the pinch-off point  $z/l_v, t/t_v \approx 1$ . For the relatively low viscosity of the system MIXD the reference values are equal to  $2.23 \mu\text{m}$  and  $0.44 \mu\text{s}$ , respectively (see Table 1). Comparing Fig. 13a with the observations of the pinch-off region (Fig. 3), we see that the both shape and time scales of the phenomena are only in qualitative agreement with the prediction. At time  $1.3 \mu\text{s}$  before the breakup Fig. 13a shows a thin, about  $30 \mu\text{m}$  long structure, connecting the jet and the droplet. In the corresponding image of Fig. 3 this can be identified as the previously discussed micro-thread. Also predicted and measured retraction velocities of the jet tip shown in the same figures seem to agree relatively well for time  $1.3 \mu\text{s}$  after breakup. At a larger distance from the singularity point the predicted jet shape diverges rapidly. This is not very surprising, as the validity of the model is limited only to a very small region close to the breakup point. An increase of liquid viscosity expands this region. Fig. 13b shows the calculated shapes of the thread, to be compared with Fig. 5, where the results of experiments performed for higher viscosity (MIXE) are displayed.

According to the definition of  $\phi(\xi)$ , the jet tip should have an elongated conical shape as it can be seen in Fig. 13b. However, in the experiment, the angle of the thread cone is smaller than that predicted by the model. The micro-thread forms a rather long, thin cylinder, which at some distance from the droplet rapidly changes its diameter and merges the macro-thread. It demonstrates the limits of the model, which cannot predict the macro-thread and becomes inadequate for  $z \geq l_v$ , i.e. about 0.1 mm from the breakup point. The comparison of corresponding drawing and jet image displayed for time 8.3  $\mu\text{s}$  after the breakup shows that the retraction velocity of the micro-thread has been predicted relatively well by the model.

The comparison of the calculated and observed breakup region for highly viscous liquid (system GLY3) is shown in Fig. 7. Now, the full length of the micro-thread fulfils the condition  $z/l_v \approx 1$ . In fact the predicted jet shape practically overlaps the observed boundaries of the thread. However, severe discrepancies are observed at the droplet side, where the observed shape diverges much faster than the predicted one. This is probably an effect of the droplet itself: adjusting to a spherical shape cannot be described by the asymptotic model.

From the above comparison it follows then, that the asymptotic model given by Eggers (1993) (Eggers and Dupont, 1994; Eggers, 1995) properly describes the shape of jet only around the singularity point. Consequently, the model gives the correct asymptote for the jet diameter, as demonstrated in Fig. 12. The comparison of both diverging ends of the thread with experimental observations shows severe discrepancies. Also the kinematics of the thread contraction after the pinch-off shows for higher viscosities discrepancies difficult to interpret. Predicted increase of the retraction velocity in function of viscosity could not be confirmed and rather opposite relation was observed.

#### 4. Final discussion

As we mentioned earlier, modeling the pinch-off process becomes very difficult when we approach the point of singularity, where the jet diameter tends to zero. A practical question arises: what is the physical limit of the jet thinning? Is it of the size of molecules? The molecular dynamic simulation by Koplik and Banavar (1993) indicates that on scales of the present experiment the molecular effects are negligible. It is interesting to note that according to their model the Navier–Stokes equations surprisingly extend their validity at least down to 100 Å and  $10^{-10}$  s in length and time scales. Hence, their use for direct numerical simulation of the pinch-off problem seems to be justified. In any case, the present observations have shown that the liquid neck breaks up long before reaching the molecular size. Hence, there must be some other mechanism determining the minimum jet size.

The jet breaks up when the micro-thread approaches its limiting size of  $\approx 1 \mu\text{m}$ . This limit seems to be independent of the parameters of the liquid; the region of the jet thinning simply extends in length with increasing viscosity. From the optical observations one cannot completely dismiss a possibility that the micro-thread will thin again to create the next nano-thread cascade. However, the present observations do not give any justification for such a hypothesis. Observations of long, almost uniform micro-threads have shown that these liquid structures always become unstable when their diameter falls down below one micrometer.

One may propose several hypotheses to explain this stability limit. The most straightforward would be the idea that the presence of the external gas limits the thinning process. In fact, parallel flow along a cylinder is characterized by a viscous shear stress growing as  $1/r$  per unit area of its surface. Hence,

at some critical jet diameter the effect of the external gas may overcome the surface tension and the cylindrical shape of the thread may become unstable. The appearance of the several small swellings, before the micro-thread breaks, argues against this hypothesis. The experiment performed for the oil jet at low ambient pressure (system G29) effectively rules out this idea. Although the dynamic effects of the external gas were considerably minimized at 100 Pa, the observed scenario of the pinch-off process remained unchanged. In both cases investigated, i.e. at atmospheric pressure (100 kPa) and at low gas pressure (100 Pa), the thin micro-thread exhibited similar forms of instability (several small swellings), and it broke up at one or more points, creating micro-satellites. This experiment performed for the low vapour pressure oil rules out another suggestion: that it is the evaporation of the micro-thread which initiates its final breakup.

There are also thermal fluctuations which could be taken into account as a possible breakup agent. Is their scale large enough to limit the thinning of the micro-thread to micrometer size? To justify such an idea one would have to change drastically the scale of the thermal fluctuations, e.g. by performing a low-temperature experiment with liquid nitrogen. A thermal threshold length scale (Eggers, 1995), which was identified by Brenner et al., (1994), does not seem to be appropriate, as its dependence on viscosity implies one order of magnitude increase of the micro-thread diameter between mixtures MIXE and GLY3. In fact, the molecular simulations of Koplík and Banavar (1993) indicate that macroscopic flow structures of threads and droplets seem to be very insensitive to the imposed thermal noise. In any case, at the moment the explanation of the observed limit of the micro-thread thinning process is still lacking.

## 5. Summary

The experiments have shown, that over the wide range of variation of liquid parameters (mainly viscosity) included in this study, the process of droplet separation from the liquid jet has common characteristics. Initially the tip of the jet close to the droplet becomes convergent, elongates, and forms the first structure, called the macro-thread. This macro-thread was usually considered in previous experiments to be the final form of the tip, which suddenly separated from the droplet and created a satellite. The present experiments show that, before this happens, a new cascade-like thinning of the tip begins, creating the second, thin micro-thread between the macro-thread and the droplet. The maximum length of the micro-thread is strongly dependent on liquid viscosity, varying from micrometers to several millimetres. However, the diameter of the micro-thread which is observed before rupture is almost constant. In addition, the retraction velocity after the breakup exhibits relatively small variations with viscosity.

The maximum length of the micro-thread can be correlated using Eggers' (1993) viscous length  $l_v$ . Also, the asymptotic variation of the thread diameter before pinch-off, confirms predictions of his model. However, the final thread diameter, the point of the pinch-off, and the retraction velocity cannot be predicted properly.

Our experiments cannot fully confirm Eggers' model, but its predictions certainly give qualitatively correct characteristics of the pinch-off process. The model assumption about a local character of the droplet separation process is correct. In practice, the pinch-off process seems to be completely insensitive to the external initial conditions like jet velocity, diameter or perturbation amplitude. Discrepancies in the predicted velocities and in the final thread diameters indicate that the proposed

asymptotic description has a limited validity. This is perhaps due to the fact that the model assumes a different scenario of the final pinch-off. Hence, it is still necessary to look for a theoretical description which can fully describe the hydrodynamics of the breakup process.

## Acknowledgements

The author thanks his colleagues in the Max-Planck-Institut for their hospitality and support, with the special thanks to Winfried Hiller. He also thanks Jens Eggers for the stimulation and help in providing necessary details of the asymptotic model.

## References

- Becker, E., W.J. Hiller and T.A. Kowalewski (1991) Experimental and theoretical investigation of large amplitude oscillations of liquid droplets, *J. Fluid Mech.* 231, 189–210.
- Bogy, D.B. (1979) Drop formation in a circular liquid jet, *Annu. Rev. Fluid Mech.* 11, 207–228.
- Brenner, M.P., X.D. Shi and S.R. Nagel (1994) Iterated instabilities during droplet fission, *Phys. Rev. Lett.* 73, 3391–3398.
- Chaudhary, K.C. and T. Maxworthy (1980a) The nonlinear capillary instability of a liquid jet. Part 2. Experiments on jet behaviour before droplet formation, *J. Fluid Mech.* 96, 275–286.
- Chaudhary, K.C. and T. Maxworthy (1980b) The nonlinear capillary instability of a liquid jet. Part 3. Experiments on satellite drop formation and control, *J. Fluid Mech.* 96, 287–297.
- Chaudhary, K.C. and L.G. Redekopp (1980) The nonlinear capillary instability of a liquid jet. Part 1. Theory, *J. Fluid Mech.* 96, 257–274.
- Cram, L.E. (1984) A numerical model of droplet formation, in: *Computational Techniques and Applications: CTAC-83*, eds. J. Noye and C. Fletcher (Elsevier, North-Holland) 182–188.
- Crane, L., S. Birch and P.O. McCormack (1964) The effect of mechanical vibration on the breakup of a cylindrical water jet in air, *Brit. J. Appl. Phys.* 15, 743–750.
- Crane, L., S. Birch and P.O. McCormack (1965) An experimental and theoretical analysis of cylindrical jets subjected to vibration, *Brit. J. Appl. Phys.* 16, 395–408.
- Donnelly, R.J. and W. Glaberson (1966) Experiment on capillary instability of a liquid jet, *Proc. Roy. Soc. Lond. A* 290, 547–556.
- Eggers, J. (1993) Universal pinching of 3D axisymmetric free-surface flow, *Phys. Rev. Letters* 71, 3458–3460.
- Eggers, J. (1995) Theory of drop formation, *Phys. Fluids A* 7, 941–953.
- Eggers, J. and T.F. Dupont (1994) Drop formation in a one-dimensional approximation of the Navier-Stokes equation, *J. Fluid Mech.* 262, 205–221.
- Goedde, E.F. and M.C. Yuen (1970) Experiments on liquid jet instability, *J. Fluid Mech.* 40, 495–511.
- Hiller, W.J. and T.A. Kowalewski (1987) Eine einfache Hochgeschwindigkeits-kamera mit CCD-Sensor (Max-Planck-Institut für Strömungsforschung, Bericht 8/1987, Göttingen).
- Hiller, W.J. and T.A. Kowalewski (1989a) Surface tension measurements by the oscillating droplet method, *Phys. Chem. Hydrodyn.* 11, 103–112.
- Hiller, W.J. and T.A. Kowalewski (1989b) Application of the frame transfer charge-coupled device for high speed imaging, *Optical Eng.* 28, 197–200.
- Hiller, W.J., T.A. Kowalewski and B. Stasicki (1989) Schnelle Bildaufzeichnung mit CCD-Kameras und gepulsten LEDs, *Laser und Optoelektronik* 21, 64–68.
- Hiller, W.J., T.A. Kowalewski, V. Llorach Forner, B. Stückrad and M. Behnia (1992) Charge-coupled devices in flow visualisation, in: *Proc. 6th Int. Symp. on Flow Visualisation, Yokohama 1992*, eds. Y. Tanida and H. Miyashiro (Springer, Berlin) 695–699.
- Hiller, W.J., T.A. Kowalewski and Th. Tatarczyk (1993) High speed frame transfer CCD, in: *Proc. 20th Int. Congr. of High Speed Photography and Photonics, Victoria 1992, SPIE Vol. 1801* (SPIE Washington) 595–601.

- Hiller, W., H.-M. Lent, G.E.A. Meier and B. Stasicki (1987) A pulsed light generator for high speed photography, *Exp. Fluids* 5, 141–144.
- Kalita, W. (1975) Drop formation in a transient régime of dispersion, *Arch. of Mech.* 27, 649–663.
- Keller, J.B. and M.J. Miksis (1983) Surface tension driven flows, *SIAM J. Appl. Maths.* 43, 268–277.
- Koplik, J. and J.R. Banavar (1993) Molecular dynamics of interface rupture, *Phys. Fluids A* 5, 521–536.
- Peregrine, D.H., G. Shoker and A. Symon (1990) The bifurcation of liquid bridges, *J. Fluid Mech.* 212, 25–39.
- Plateau, J.A.F. (1873) *Statique expérimentale et théorique des liquides soumis aux seules forces moléculaires* (Gauthiers-Villars, Paris) Vol. II, p. 231.
- Rayleigh, J.W.S. (1878) On the instability of jets. *Proc. Lond. Math. Soc.* 10, 4–13.
- Schultz, W.W. (1987) Slender viscoelastic fiber flow, *J. of Rheology* 31, 733–750.
- Schultz, W.W. and S.H. Davis (1982), One-dimensional liquid fibers, *J. of Rheology* 26, 331–345.
- Shi, X.D., M.P. Brenner and S.R. Nagel (1994) A cascade of structure in a drop falling from a faucet, *Science* 265, 219–222.
- Sterling, A.M. and C.A. Sleicher (1975) The instability of capillary jets, *J. Fluid Mech.* 68, 477–495.
- Stone, H. (1994) Dynamics of drop deformation and breakup in viscous fluids, *Annu. Rev. Fluid Mech.* 26, 65–102.
- Vassallo, P. and N. Ashgriz (1991) Satellite formation and merging in liquid jet breakup, *Proc. R. Soc. Lond. A* 433, 269–286.
- Weber, C. (1931) Zum Zerfall eines Flüssigkeitsstrahles, *ZAMM* 11, 135–154.
- Yarin, A.L. (1993) *Free liquid jets and films: hydrodynamics and rheology* (Longman Sci. and Techn., Essex).
- Ziabicki A. and H. Kawai, eds. (1985) *High-speed fiber spinning: science and engineering aspects* (Wiley, New-York).